POLITECNICO DI TORINO
Repository ISTITUZIONALE

Frequency combs in III-V/SiN integrated hybrid lasers with narrowband mirror

Original
Frequency combs in III-V/SiN integrated hybrid lasers with narrowband mirror / Rimoldi, C., Columbo, L.L., Gioannini, M.. - ELETTRONICO. - 12905:(2024), pp. 1-3. (SPIE Photonics West OPTO 2024 San Francisco (USA) 27 January - 1 February 2024) [10.1117/12.3003710].

Availability:
This version is available at: 11583/2987678 since: 2024-04-09T09:18:35Z

Publisher:
SPIE

Published
DOI:10.1117/12.3003710

Terms of use:

This article is made available under terms and conditions as specified in the corresponding bibliographic description in the repository

Publisher copyright
SPIE postprint/Author's Accepted Manuscript e/o postprint versione editoriale/Version of Record con

Copyright 2024 Society of PhotoOptical Instrumentation Engineers (SPIE). One print or electronic copy may be made for personal use only. Systematic reproduction and distribution, duplication of any material in this publication for a fee or for commercial purposes, and modification of the contents of the publication are prohibited.

(Article begins on next page)

17 October 2026

Frequency combs in III-V/SiN integrated hybrid lasers with narrowband mirror

Cristina Rimoldi[a], Lorenzo L. Columbo[a], and Mariangela Gioannini[a]

[a]Dipartimento di Elettronica e Telecomunicazioni, Politecnico di Torino, Corso Duca degli Abruzzi 24, 10129 Turin, Italy

ABSTRACT

We address the dynamics of a III-V/SiN external cavity hybrid laser with a frequency-selective mirror. Simulations through a set of time-delayed algebraic equations accounting for the narrowband SiN mirror reflectivity demonstrate that CW instability occurs when relaxation oscillations become resonant with the beating between longitudinal modes. In the CW unstable regime, we observe the emergence of frequency combs due to four wave mixing, characterized by a modulation of amplitude and frequency. We then characterize the resulting combs in terms of achievable bandwidth. These results are also confirmed through a more accurate time-domain traveling wave model.

Keywords: Silicon Photonics, hybrid integrated lasers, optical frequency combs

1. INTRODUCTION

Integrated laser sources within Silicon Photonic (SiPh) platforms allow for low-cost devices with applications in data centers. In this context, Silicon Photonic circuits including microring resonators are often used to the purpose of reducing the single-mode linewidth,[1] since narrow bands are usually required in the context of high-speed optical transceivers. On the other hand, the introduction of such microring configurations (see e.g. Fig. 1(a)) introduces an effective reflectivity from the SiPh circuit that is selective in frequency, with an FWHM that can be as narrow as a few GHz. As a result, the SiPh circuit effective length increases for narrowband reflectivities, allowing for the laser longitudinal modes to be closer in frequency. While much work has been dedicated to the stability and characterization of single-mode solutions, only a few papers have reported on the emergence of multimode regimes.[2,3] In this contribution, we discuss such a topic from a theoretical and numerical perspective and we illustrate how the combined effect of modal competition, a non-null α factor, and the undamping of relaxation oscillations result in the instability of the CW solution and the emergence of multimode regimes. Optical Frequency Comb (OFC) generation is then made possible due to mode proliferation and mode locking, provided by four-wave mixing. The resulting comb is preliminary characterized in terms of -20 dB bandwidth, demonstrating comb spans up to 90 GHz.

2. MODELING AND RESULTS

In Fig. 1(a) we illustrate the studied device. It consists of a III-V Reflective Semiconductor Optical Amplifier (RSOA) that is edge-coupled to a SiN circuit, including two coupled rings, providing a narrowband reflectivity via Vernier effect. The SiN circuit includes a Spot Size Converter (SSC) and a Phase Section (PS) that allows to detune the frequency of single-mode emission with respect to the peak of the SiN mirror effective reflectivity by an amount $\Delta\nu$, due to a phase shift $\Delta\phi$. The power P_{out} is extracted through an output coupler. The ring radii are about 100 μm, the RSOA has a length $L = 1$ mm, and the overall length of the bus waveguide from the SSC to the ring input measures about 1.5 mm.

We describe this laser through the following set of delayed algebraic rate equations, based on the approach illustrated by Tromborg et al.[4] and adapted to include the effect of the narrowband reflectivity from the two

Further author information: (Send correspondence to C. Rimoldi.)
C. Rimoldi: E-mail: cristina.rimoldi@polito.it

Novel In-Plane Semiconductor Lasers XXIII, edited by Alexey A. Belyanin, Peter M. Smowton,
Proc. of SPIE Vol. 12905, 129050I · © 2024 SPIE · 0277-786X · doi: 10.1117/12.3003710

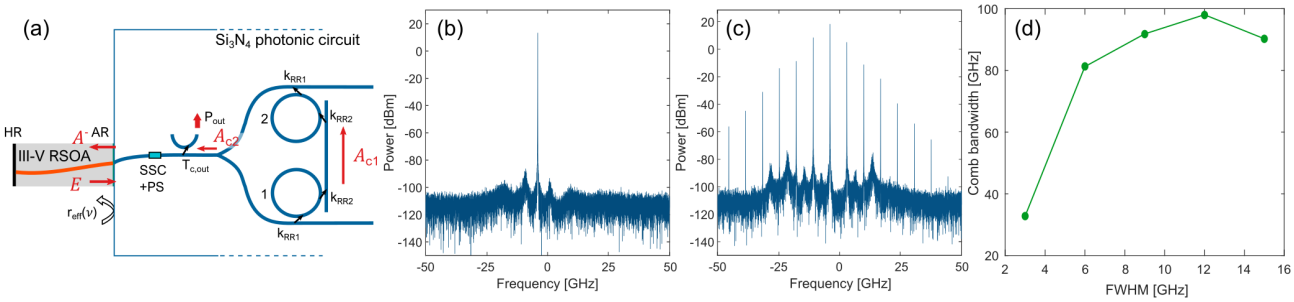

Figure 1. (a) Schematics of the studied device. (b,c) Optical spectra at $I = 100\,\text{mA}$ (b) and $I = 280$ mA (c). (d) Trend of the -20 dB OFC bandwidth as a function of $|r_{eff}|^2$ FWHM.

coupled rings.[5] The model is valid in the neighborhood of the CW solutions, under the approximation of spatially averaging the optical power along the RSOA.

$$E(t) = \frac{e^{i(\omega_s-\omega_0)\tau_{in}}\exp f(\omega_s,N_s)}{r_{eff}(\omega_s)}A^-(t-\tau_{in}) + F(t) \tag{1}$$

$$\frac{\mathrm{d}A_{c1}(t)}{\mathrm{d}t} = \gamma_{c1}t_{SSC}\sqrt{1-T_{c,out}}E(t-\tau_{in,SiN}/2)e^{-i\frac{\Delta\phi}{2}} - \gamma_{t1}A_{c1}(t) \tag{2}$$

$$\frac{\mathrm{d}A_{c2}(t)}{\mathrm{d}t} = \gamma_{c2}A_{c1}(t) - \gamma_{t2}A_{c2}(t) \tag{3}$$

$$\frac{\mathrm{d}N(t)}{\mathrm{d}t} = \frac{\eta_i I}{qV} - \frac{N(t)}{\tau_N} - v_g g_N \ln\left(\frac{N(t)}{N_0}\right)\sigma\frac{|E(t)|^2}{V} \tag{4}$$

with

$$A^-(t-\tau_{in}) = t_{SSC}\sqrt{1-T_{c,out}}e^{-i\frac{\Delta\phi}{2}}A_{c2}(t-\tau_{in}-\tau_{in,SiN}/2) \tag{5}$$

$$f(\omega_s,N_s) = \frac{1}{\tau_{in}}\int_{t-\tau_{in}}^{t} L\left(1+i\alpha\frac{\omega_s}{\omega_0}\right)g_N\ln\left(\frac{N(\bar{t})}{N_s}\right)\mathrm{d}\bar{t} \tag{6}$$

$$\tag{7}$$

and effective reflectivity

$$r_{eff}(\omega) = \frac{\gamma_{c1}\gamma_{c2}t_{tr}^2}{(\gamma_{t1}+i\Delta\omega)(\gamma_{t2}+i\Delta\omega)}e^{-i\Delta\phi}e^{-i\Delta\omega\tau_{in,SiN}}\,, \tag{8}$$

In Eq. (1), $E(t)$ is the slowly varying envelope of the field exiting the RSOA at the AR-coated facet, $A_{c1}(t)$ is the field at the drop port of the first ring, $A_{c2}(t)$ is the field after propagation in the second ring, and $N(t)$ is the carrier density in the RSOA. ω_s is the angular frequency of the CW solution under study (with corresponding carrier density N_s), ω_0 is the reference angular frequency, matching the peak of the effective reflectivity, and $\Delta\omega = \omega - \omega_0$. The RSOA roundtrip time is τ_{in}, and $\tau_{in,SiN}$ is the time delay related to the bus waveguide sections of the SiPh circuit. The spot size converter transmission coefficient is t_{ssc} and $T_{c,out}$ is the power transmission coefficient of the output coupler. $F(t)$ is a Langevin stochastic term accounting for spontaneous emission. In Eq. (2-3), $\gamma_{c1,2}$,$\gamma_{t1,2}$ are, respectively, the rates at which the electric field couples into the ring from the bus waveguide and the rate at which the electric field is lost, due to coupling out of the bus waveguide and waveguide losses.[6] Finally in Eq. (4), η_i is the internal quantum efficiency, I is the bias current, q is the electron charge, V is the volume of the active region, v_g is the group velocity, g_N is the modal gain, N_0 is the transparency carrier density, and σ is a coefficient accounting for the spatial average of the optical field along the RSOA. The effective reflectivity in Eq. (8) has the typical shape of the product of two Lorentzian functions.[5] Parameter values and additional considerations on the model and its derivation have been previously reported.[5]

While the model has already been employed to characterize the laser feedback resilience[7] and the stability of CW solutions,[5] in the following we focus on the mechanism giving rise to the self-generation of OFCs.

In Fig. 1(b), we display the laser optical spectrum resulting from our dynamical simulations at a bias current I=100 mA, $|r_{eff}|^2$ FWHM=6 GHz, and a detuning, due to the phase section, of -4 GHz with respect to the effective reflectivity peak at ω_0. Apart from the main peak, centered around $\Delta\nu = \Delta\omega/2\pi = -4$ GHz, we observe two secondary peaks associated to the relaxation oscillation sidebands. The CW unstable regime is triggered by the efficient conversion of phase noise into intensity noise, aided by the α factor, which enhances again the phase noise: a mechanism resulting in undamped relaxation oscillations. When the frequency of relaxation oscillations becomes resonant with the frequency separation between two possible CW solutions then a multimode regime can occur.[5] Following such a mechanism of destabilization, an OFC can self-generate due to four wave mixing and mode proliferation occurs as an effect of parametric gain and phase locking between comb lines. In Fig. 1(c), we report the resulting comb at $I = 280$ mA.
As anticipated, the model of Eq. (1-4) is useful in order to address the main mechanism giving rise to CW instability but it can become less accurate in the description of the laser behavior far from the CW solution. For this reason, for the characterization of the resulting comb at higher current, we employed a Time-Domain Traveling Wave (TDTW) model accounting in particular for the carrier density and electric field spatial distribution within the RSOA, which will be the subject of a future publication. As a preliminary result, we display in Fig. 1(d) the maximum -20 dB comb bandwidth achievable for varying detuning of the phase section at the fixed current of $I = 300$ mA. Here, we observe a maximum achievable -20 dB bandwidth of about 90 GHz for a $|r_{eff}|^2$ FWHM=12 GHz. The trend of Fig. 1 can be explained as follows: small FWHM are effective in reducing the comb span due to their narrow band, on the other hand the saturation for increasing FWHMs is due to the fact that more longitudinal modes, beyond the four-wave mixing locking range can reach threshold, giving rise to more complex multimode dynamical regimes instead of OFCs.

3. CONCLUSIONS

We addressed the mechanism giving rise to the CW instability in an integrated hybrid laser featuring a narrowband effective reflectivity. The self-generation of OFCs is illustrated and the resulting combs are characterized in terms of -20 dB bandwidth. Future work will be dedicated to a more detailed characterization in terms of phase and amplitude noise of the comb lines, as well as the study of nonlinear effects on the OFC.

ACKNOWLEDGMENTS

This work was partially supported by the European Union under the Italian National Recovery and Resilience Plan (PNRR) of NextGenerationEU, partnership on "Telecommunications of the Future" (PE00000001 - program "RESTART"). CR acknowledges funding from research contract no. [32-I-13427-1] (DM 1062/2021) funded within the Programma Operativo Nazionale (PON) Ricerca e Innovazione of the Italian Ministry of University and Research.

REFERENCES

[1] Tran, M. A., Huang, D., and Bowers, J. E., "Tutorial on narrow linewidth tunable semiconductor lasers using Si/III-V heterogeneous integration," *APL Photonics* **4**(11), 111101 (2019).

[2] Mak, J., van Rees, A., Fan, Y., Klein, E. J., Geskus, D., van der Slot, P. J. M., and Boller, K.-J., "Linewidth narrowing via low-loss dielectric waveguide feedback circuits in hybrid integrated frequency comb lasers," *Opt. Express* **27**, 13307–13318 (Apr 2019).

[3] Huang, D., Tran, M. A., Guo, J., Peters, J., Komljenovic, T., Malik, A., Morton, P. A., and Bowers, J. E., "High-power sub-khz linewidth lasers fully integrated on silicon," *Optica* **6**, 745–752 (Jun 2019).

[4] Detoma, E., Tromborg, B., and Montrosset, I., "The complex way to laser diode spectra: example of an external cavity laser strong optical feedback," *IEEE Journal of Quantum Electronics* **41**(2), 171–182 (2005).

[5] Rimoldi, C., Columbo, L. L., Bovington, J., Romero-García, S., and Gioannini, M., "Damping of relaxation oscillations, photon-photon resonance, and tolerance to external optical feedback of III-V/SiN hybrid lasers with a dispersive narrow band mirror," *Opt. Express* **30**, 11090–11109 (Mar 2022).

[6] Chrostowski, L. and Hochberg, M., [*Silicon Photonics Design: From Devices to Systems*], Cambridge University Press (2015).

[7] Rimoldi, C., Columbo, L. L., Bovington, J., Romero-García, S., and Gioannini, M., "CW emission and self-pulsing in a III-V/SiN hybrid laser with narrow band mirror," *IEEE Photonics Journal* **14**(4), 1–7 (2022).